NJC

RSC Publishing

PAPER

View Article Online
View Journal | View Issue

Cite this: *New J. Chem.*, 2013, **37**, 834

Effect of some nitrogen donor ligands on the optical and structural properties of CdS nanoparticles

Damian C. Onwudiwe,*[a] Christien A. Strydom[a] and Oluwatobi Samuel Oluwafemi[b]

Received (in Montpellier, France) 12th October 2012,
Accepted 8th January 2013

DOI: 10.1039/c3nj40924d

www.rsc.org/njc

The cadmium complex of *N*-ethyl-*N*-phenyl dithiocarbamate, **1**, and its 2,2′-bipyridine and 1,10-phenanthroline adducts, **2**, and **3**, respectively, have been used as single source precursors for the synthesis of CdS nanoparticles. The formation of CdS nanoparticles was achieved by thermal decomposition of the complexes (pyrolysis) and thermolysis in the presence of hexadecylamine – HDA (solvothermal). Scanning electron microscopy (SEM), energy dispersive X-ray analysis (EDX) and high resolution transmission electron microscopy (HRTEM) analyses were carried out to study the structural properties of the nanoparticles. Complex **1** afforded rod-shaped nanoparticles while star-shaped nanoparticles were obtained from complexes **2** and **3**. The optical property of the CdS nanoparticles was studied by UV–visible and fluorescence spectroscopy. The spectral features for the nanoparticles prepared *via* the solvothermal route were significantly sharper and blue shifted to a greater extent relative to the corresponding bulk semiconductor, compared to the observed shift in the nanoparticles prepared *via* pyrolysis. All the as-synthesized material exhibited band edge luminescence.

Introduction

Nanoparticles with size less than the exciton radius are called quantum dots, the value is usually less than 10–20 nm. They form a link between molecular and bulk states of matter.[1] As the size of a colloidal material approaches that of the molecules or atoms which form it, its physical and chemical properties are no longer those of the 'bulk' material and are instead called 'molecular'. These materials reveal new physical properties which are strongly influenced by the high proportion of atoms or molecules at their surface and form an intermediate level between an atomic or molecular and a bulk environment.[2] The primary interest in quantum dots stems from their small particle size and the impact this has on the bulk properties of the material from which they are formed.[3]

Cadmium sulphide (CdS) is one of the most important representatives of groups II–VI semiconductors, with a band gap energy of 2.42 eV (512 nm) at room temperature.[4] It possesses many excellent physical and chemical properties which have promising applications in multiple technical fields including lasers, light-emitting diodes, sensors, solar cells and in photochemical catalysis.[5–10] Several approaches have been explored towards the synthesis of nanocrystalline CdS nanoparticles, such as the microwave-solvothermal method,[11] the sonochemical route[12] and the surfactant–ligand co-assisting solvothermal method.[13] The conventional method involves the decomposition of two-component mixtures of volatile organometallic precursors, typically cadmium alkyls, and H_2S or thiophene.[14–16] Although this method leads to the formation of the desired materials, the noxious and hazardous nature of the reagents necessitates the need for a green and safer synthetic route. In this regard, the use of a single source precursor has attracted considerable attention in recent times and a variety of organo-metallic complexes have been reported for various semiconductor nanocrystals.[17–21] Because of their high surface energy, the development of a stable colloidal suspension of semiconducting nanocrystals (NCs) is highly challenging. Therefore, it is essential to use surfactants or other capping materials during the chemical process to passivate these NCs in order to prepare a well-dispersed and stable colloidal suspension in a solvent medium.

Cadmium-*N*-ethyl-*N*-phenyl dithiocarbamate, which is the precursor for the prepared adducts in this study, was observed to be insoluble in typical organic solvents such as dichloromethane and chloroform, in its initially prepared form. Thus, derivatization routes are required to make the compound soluble in order to obtain a purer compound *via* recrystallization. Although earlier reports have demonstrated that adducts

[a] *Chemical Resource Beneficiation, North-West University, Private Bag X6001, Potchefstroom 2520, South Africa. E-mail: dconwudiwe@webmail.co.za; Fax: +27 18 299 2350; Tel: +27 18 299 1068*
[b] *Department of Chemistry and Chemical Technology, Walter Sisulu University, Mthatha campus Private Bag X1, Mthatha, South Africa*

of group 12 compounds can be employed in the preparation of 12–16 semiconductor nanoparticles,[20–22] as far as the authors know there has never been any report on the use of the present Lewis base-derived cadmium compounds as precursors for CdS nanoparticles. While the thermal decomposition of these precursors does lead to formation of the metal sulphide powders, it is important to investigate the effect of different preparatory conditions on the structural and optical properties of the as-synthesized nanomaterial. Thus, we herein report the effect of an additional ligand molecule (2,2′-bipyridine and 1,10-phenanthroline) on the optical and structural morphologies of CdS nanoparticles. In addition, we also carried out a comparative study on the properties of CdS nanoparticles prepared from these compounds, in the presence and the absence of capping agent (HDA).

Experimental

Materials and methods

The following chemicals used in this study, *N*-ethyl aniline, cadmium chloride, hexadecylamine (HDA), trioctylphosphine (TOP), toluene and absolute methanol, were purchased from Aldrich. Aqueous ammonia, chloroform, 2,2′-bipyridine and 1,10-phenanthroline were obtained from Merck. All chemicals were used as received without further purification.

Absorbance and fluorescence spectroscopy

Optical measurements of the obtained solutions were carried out at room temperature on a Perkin Elmer Lambda 20 UV-Vis Spectrophotometer using a quartz cell (10 mm path). A Jobin Yvon-spex-Fluorolog-3-Spectrofluorometer with a xenon lamp (150 W) was used to measure the photoluminescence of the particles.

Electron microscopy

Samples for TEM measurements were prepared by redispersion of the obtained powdered samples in toluene and then placing a drop of the colloidal solution on a carbon coated copper TEM grid. The film on the TEM grid was allowed to dry prior to the measurement. TEM measurements were performed on a TECNAI 20 (ACI) instrument operated at an accelerating voltage of 200 kV. Scanning electron microscopy images were obtained on a Quanta FEG 250 Environmental scanning electron microscope (ESEM).

X-Ray diffraction analysis

XRD patterns of all the synthesized samples were recorded on a Bruker D8 advanced, equipped with a proportional counter, using Cu Kα radiation (λ = 1.5405 A, nickel filter). Measurements were taken at a high angle 2θ range of 20–80° using a scan speed of 0.01°, with a filter time-constant of 2.5 s per step and a slit width of 6.0 mm. EVA software was used for the analysis and the phase identification was carried out with the help of standard JCPDS.

Infra-red analysis

FT-IR spectra were recorded using the obtained solid amine capped samples after centrifugation and washings so as to remove the unassociated organic molecules. Spectra were recorded on a Bruker alpha-P FT-IR spectrometer in the 500–4000 cm^{-1} range.

Synthesis of the precursors

The precursor complexes were prepared in open air and at room temperature, and characterized as reported earlier.[23,24]

Preparation of nanoparticles

Preparation of CdS nanoparticles by pyrolysis in a furnace. A weighed quantity of a sample, compounds **1**, **2** and **3** (*ca.* 200 mg) in a quartz boat, was pyrolyzed at 350 °C in a furnace under nitrogen flow for 1–2 h. After cooling, the residue in the quartz boat was reweighed and characterized by TEM, SEM-EDX and XRD.

Preparation of CdS nanoparticles in coordinating solvent (HDA). In a three-necked flask fitted with a thermometer, hexadecylamine (HDA) (7.5 g) was degassed at 120 °C under nitrogen for 30 min with continuous stirring. The temperature was slowly raised to 180 °C and stabilized at this temperature. To this solution, 0.45 g of the precursor complex dispersed in 5 mL trioctylphosphine (TOP) was injected rapidly and the temperature dropped to 165 °C. The solution was heated up to 185 °C and maintained at this temperature for 1 h. The solution was allowed to cool to 70 °C, and excess methanol was introduced into it. The yellow precipitate that formed was collected by centrifugation followed by decantation of the supernatant liquid. The isolated solid was dispersed in toluene. The above centrifugation and isolation procedure was repeated several times for the purification of the prepared CdS nanocrystals.

Results and discussion

Synthesis

The dithiocarbamate and Lewis bases (such as 2,2′-bipyridine and 1,10-phenanthroline) are treated as an important class of compounds due to their versatile ability to bond with transition metal ions. Dithiocarbamate as the primary ligand for the synthesis of the precursor molecules offers several advantages which includes (i) the dithiocarbamate derived precursor is air-stable and can easily be synthesized at room temperature, (ii) the precursor has low decomposition temperature, (iii) its adducts with Lewis bases have enhanced volatility and undergo clean decomposition, resulting in the formation of CdS as the final residue. Furthermore, one dithiocarbamate ligand can form four S–Cd and one Lewis base can form two N–Cd coordination bonds to complete the six coordination geometry. The formation of stoichiometric CdS nanoparticles is expected by the breaking of the corresponding coordination core.[17] Thermogravimetry analysis was conducted to study the thermal behavior and suitability of the precursor for the preparation of CdS nanoparticles. The TGA and derivative of TGA (DTG) curves of the precursors showed a sharp weight loss in the

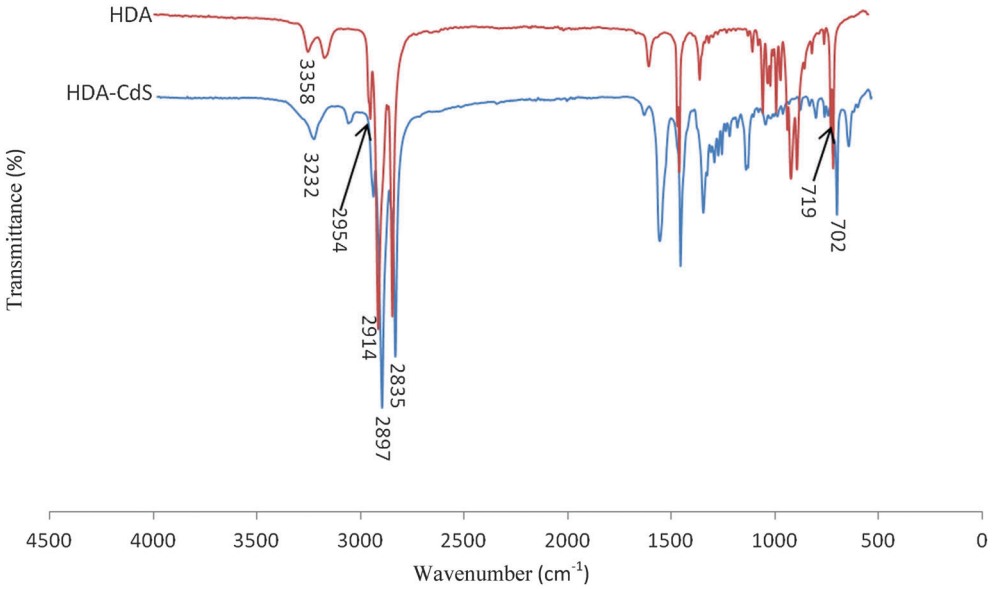

Fig. 1 FT-IR spectra of HDA and HDA-capped CdS nanoparticles.

decomposition stage which resulted in CdS residue with decomposition peak around 350 °C. Pyrolysis of the complexes **1**, **2**, and **3** was carried out at 350 °C under nitrogen flow for 1 and 2 h. In each case, the mass of the residue obtained corresponded to the stoichiometric mass of the respective metal sulfides. The compositions were further confirmed by XRD and EDX analysis.

Characterization of nanoparticles

The surface morphologies of all the CdS nanoparticles prepared by the solvothermal route were investigated using FT-IR spectroscopy to confirm the capping of the particles by hexadecylamine (HDA). Fig. 1 shows a representative spectrum. It shows the overlapped spectra of the pure HDA and the representative of the dry HDA-capped CdS nanoparticles. The FTIR spectrum of HDA shows two vibrational bands at around 2914 and 2847 cm^{-1} attributed to the CH_2 asymmetric and symmetric stretching, respectively. The band at 2954 cm^{-1} is assigned to the stretching vibration of C–H. The CH_2 rocking vibration is identified by the sharp band at 719 cm^{-1}. The gross resemblance in both spectral features and peak positions for N–H stretching vibrations in the range *ca.* 3358–3232 cm^{-1} guarantees a successful attachment of the solvent molecule onto the CdS nanocrystals. A closer observation shows that the N–H stretching peak which appeared at 3358 cm^{-1} for the pure HDA shows a shift to 3232 cm^{-1}, indicating the binding of the amine group of HDA to the nanoparticles.[25,26] Similarly, bands which correspond to the C–H stretching vibration of terminal CH_3 and CH_2 groups of the alkyl chain of the HDA molecule are blue shifted by 1–4 cm^{-1}. These relatively small shifts are due to the constraint in the molecular motion of the capping agent, which presumably resulted from its attachment on the nanoparticle surface.[27]

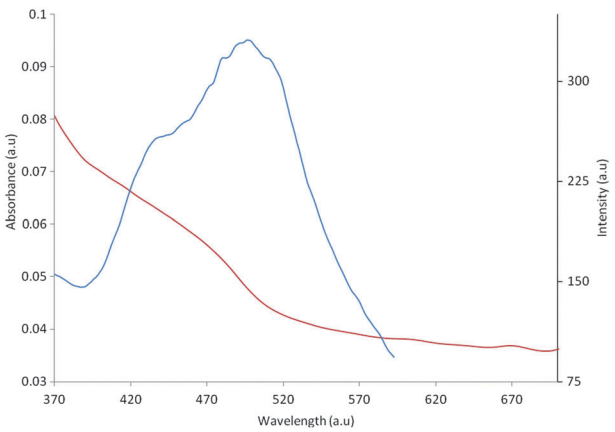

Fig. 2 (a) Absorption and (b) emission spectra of CdS nanoparticles obtained by thermolysis of complex **1** in hexadecylamine at 185 °C.

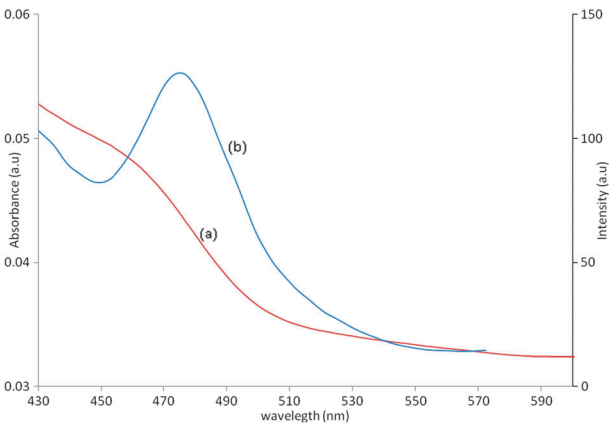

Fig. 3 (a) Absorption and (b) emission spectra of CdS nanoparticles obtained by thermolysis of complex **2** in hexadecylamine at 185 °C.

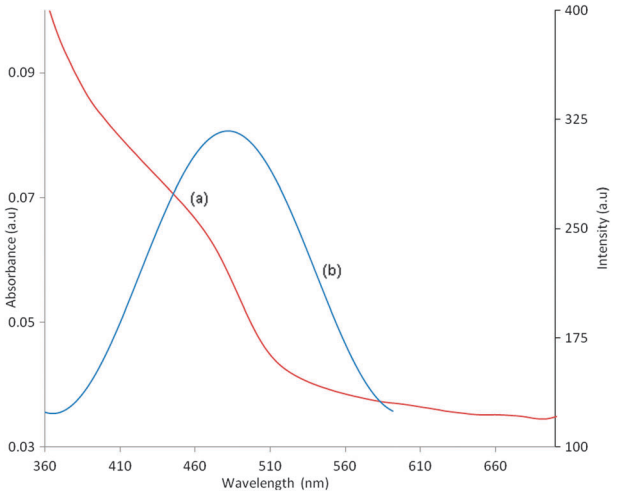

Fig. 4 (a) Absorption and (b) emission spectra of CdS nanoparticles obtained by thermolysis of complex **3** in hexadecylamine at 185 °C.

The UV–Vis spectra shown in Fig. 2(a)–4(a) display the typical shoulders of the nanometer-sized CdS at 492, 481 and 492 nm for the samples obtained from **1**, **2**, and **3** ,respectively, which are absent in the samples obtained *via* pyrolysis in the furnace (Fig. 5). This observation could be ascribed to the surface passivations by the organic material which reduces surface effects and enhances the exciton effects.[28] The surface states result from defects and dangling bonds. Thus, in the absence of a capping group, there is no carrier confinement. The as-synthesized materials, *via* the solvothermal route, show absorption peaks which are blue shifted in relation to the bulk CdS (512 nm, 2.42 eV), indicating the quantum confinement effect.[29] By using the method described by Fu *et al.*, the band gap energy corresponding to this absorption was obtained as 2.52, 2.58 and 2.52 eV for CdS nanoparticles prepared from precursor complexes **1**, **2**, and **3**, respectively.[30] In fluorescence spectroscopy, the absorption of light could either result in an electron–hole (e^-–h^+) pair or an exciton that either undergoes radiative band gap or near band gap recombination with a characteristic intensity. The photoluminescence (PL) band of the sample from complex **1** is composed of two peaks: one at 497 nm and a weak shoulder peak at around 437 nm. The emission maxima peaks are at around 475 and 483 nm for samples obtained from **2**, and **3**, respectively. For CdS nanoparticles, peaks below 500 nm are bound to be the exciton emission.[31] The effects of the absence of a capping group on

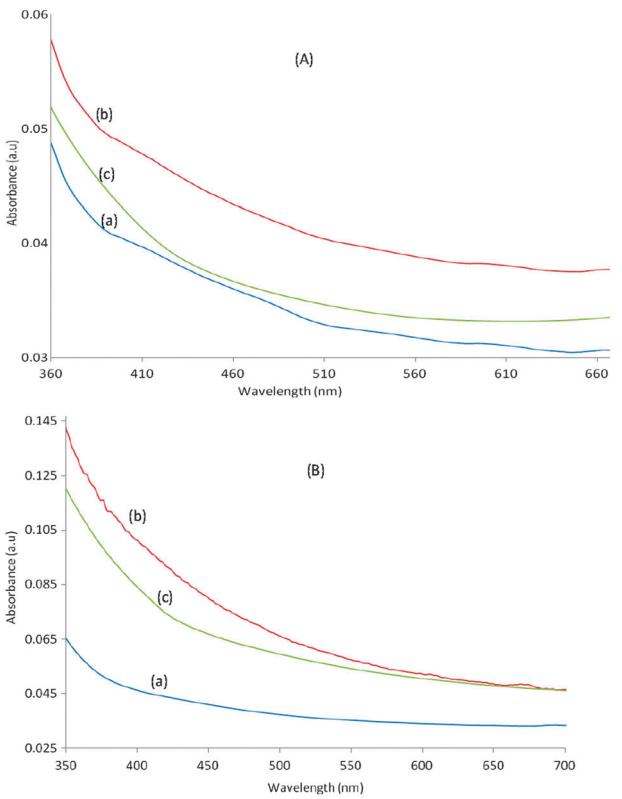

Fig. 5 Absorption spectra of CdS nanoparticles obtained by the pyrolysis of (a) complex **1**, (b) **2**, and (c) **3**, respectively, in a furnace at 350 °C under nitrogen flow for (A) 1 h, and (B) 2 h.

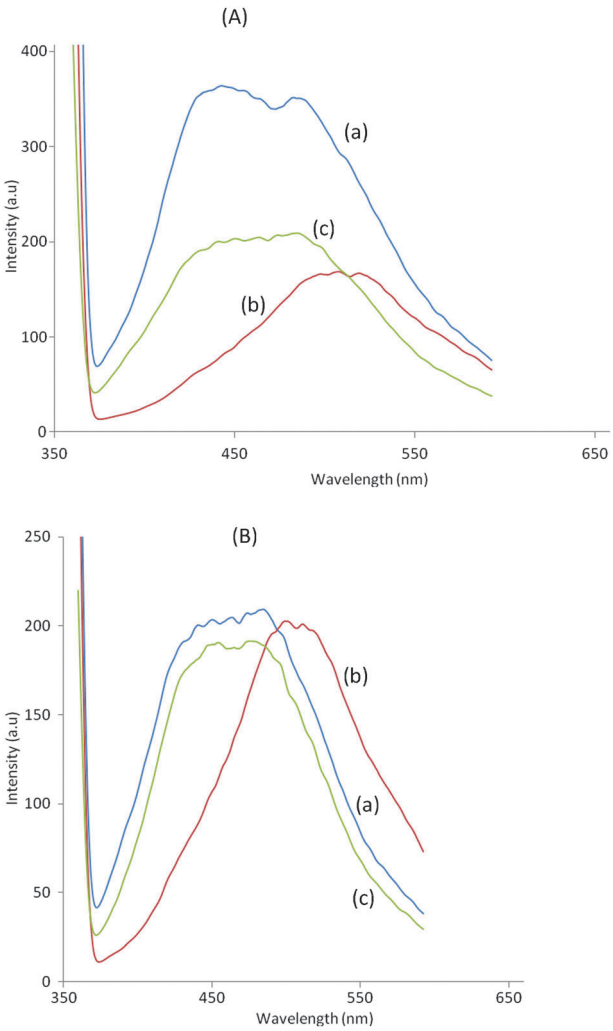

Fig. 6 Emission spectra of CdS nanoparticles obtained by the pyrolysis of (a) complex **1**, (b) **2**, and (c) **3**, respectively, in a furnace at 350 °C under nitrogen flow for (A) 1 h and (B) 2 h.

the optical behavior of the CdS nanoparticles are evident in the absorption and emission spectra of the samples obtained *via* pyrolysis in a furnace (Fig. 5 and 6). The fluorescence spectra of the grown CdS samples [Fig. 2(b)–4(b)] demonstrate that the hexadecylamine modifies the shape and size of the nanoparticles, and also enhances the photoluminescence peak intensity. Singh *et al.* demonstrated that in the synthesis of nanocrystalline CdS, increasing the capping agent concentration enhances the photoluminescence peak intensity while the peak intensity decreases with increasing annealing temperature.[32] In group II–VI capped nanoparticles, an optically excited charge carrier emits light by band-to-band and band-to-defect recombination processes.[33] Comparing the PL spectra of the uncapped nanoparticles (Fig. 6A and B) pyrolysed for 1 and 2 h, respectively, it was found that an increase in the pyrolysis time led to a relatively narrower band and a slight blue shift (5–10 nm) in the emission maxima, which may be due to reduced particle size and particle size distribution. Several reports on the PL of CdS nanocrystallites show that the photoluminescence depends on the particle size and also on the method of preparation.[34–37] A shift in the absorption edge is also noticed in the UV-Vis spectra after 2 h (Fig. 5B). Thus, in the absence of a solvent and a capping group, the complexes decomposed with non-uniform morphology, whereas in the presence of a coordinating solvent, the coordinating ligand helped in passivating the surface of the particles and improved its uniformity.

TEM and HRTEM images of CdS nanoparticles obtained by thermolysis of complexes **1** and **2** in HDA at 185 °C are shown in Fig. 7A and B. The images reveal that the particles from complex **1** are nanorods with an average length of 15 nm and a diameter of 4 nm, while particles from complex **2** are tripods. Each arm of the tripods ranged in length from 20–30 nm with diameters of 5–6.5 nm. Similar tripods were observed in the nanoparticles from complex **3**, with shorter length and diameter. Although the synthesis of the CdS nanocrystals was carried out under the same synthetic conditions of temperature and the ratio of capping groups to precursor molecules, exclusive formation of one dimensional CdS rods was observed from complex **1** while the introduction of 2,2-bipyridine (**2**) and 1,10-phenanthroline (**3**) into the precursor molecule facilitated the formation of tripods. Similar observations were made in the thermolysis of cadmium complexes of alkyl-substituted thioureas, where temperature was used as the major thermodynamic parameter to influence the morphology of CdS nanoparticles from spherical shape (at lower temperature, 100–150 °C) to rods and

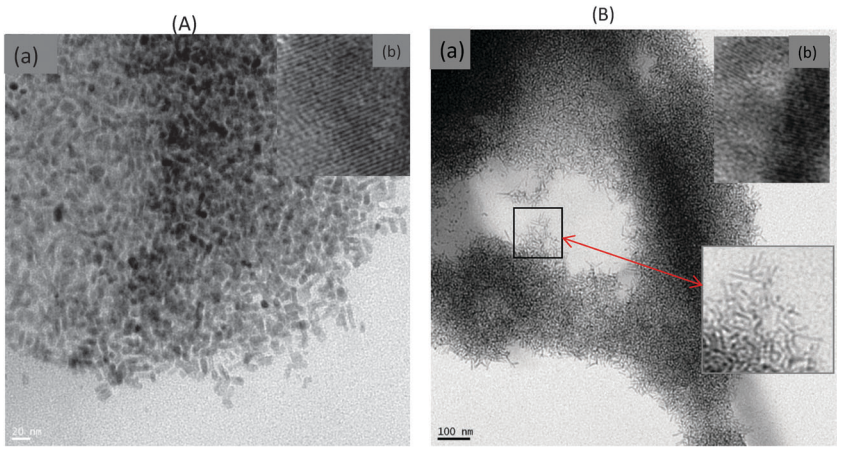

Fig. 7 (a) TEM and (b) HRTEM (inset) of nanoparticles synthesized from the thermolysis of (A) complex **1** and (B) **2** in hexadecylamine at 185 °C for 45 min.

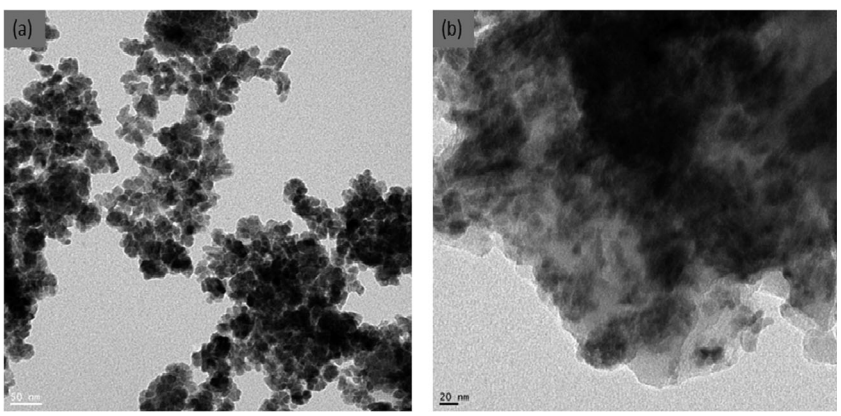

Fig. 8 TEM images of nanoparticles synthesized from pyrolysis of (a) complex **1** and (b) **2** at 350 °C for 1 h under nitrogen flow.

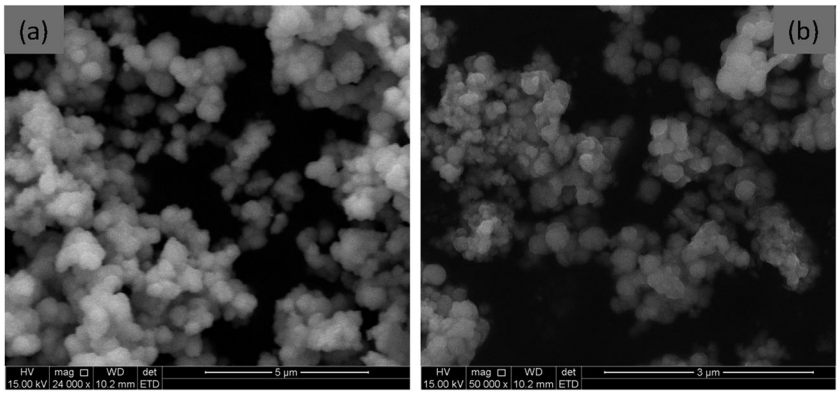

Fig. 9 SEM images of CdS nanoparticles obtained by the pyrolysis of (a) complex **1** and (b) **2** ,respectively, in a furnace at 350 °C under nitrogen flow for 1 h.

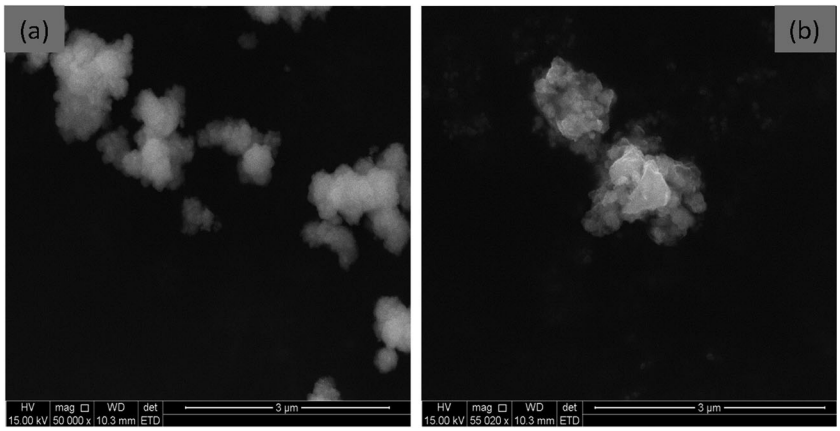

Fig. 10 SEM images of CdS nanoparticles obtained by the pyrolysis of (a) complex **1** and (b) **2** ,respectively, in a furnace at 350 °C under nitrogen flow for 2 h.

tripods (at increased temperature).[38] Star-shaped nanocrystals are seen as the transient species between isotropic zero-dimensional and anisotropic one-dimensional shapes and are usually obtained at an intermediate growth temperature.[39] Nanoparticles prepared under different conditions are known to show different phases and sizes as a result of the differences in their nucleation mechanisms.[40] TEM and HRTEM images of the nanoparticles synthesized from pyrolysis of complexes **1** and **2** at 350 °C for 1 h are shown in Fig. 8A and B. The nanoparticles formed a set of agglomerates with no definite crystalline edges. Synthesis in a surfactant medium offers several synthetic advantages such as facial separation between nucleation and growth stages, the control of growth parameters and protection of the nanoparticles from agglomeration, because the surfactant molecule dynamically binds to the crystal surface during the nucleation and growth. It is likely that in the present circumstances, agglomerates were obtained owing to high surface reactivity of the different nanoparticles. However, different mechanisms of decomposition of the precursor molecules under the furnace heat resulted in the variation of the morphology. It was difficult to determine the sizes of the nanoparticles from HRTEM images as the particles tend to agglomerate rapidly.

Heating duration may affect the structure of the nanocrystallites. The effect of the heating duration is expected to reflect on the surface morphology of the particles. To study the dependence of the surface morphology of the CdS upon duration of heating, the SEM images were taken for the CdS nanoparticles heated for different durations. Fig. 9 and 10 show the SEM images of the pyrolysed complexes **1** and **2** obtained at 350 °C, after 1 h and 2 h, respectively. A modification of the surface morphology of the CdS nanoparticles is evident from the SEM images. Fig. 9(a) and (b) show that the particles are spherical and possess a smooth surface with an average size of 460 and 270 nm, respectively. An increase in the duration of pyrolysis (keeping temperature fixed, 350 °C) resulted in a decrease in size with less distinct edges due to agglomeration of the particles (Fig. 10). Size determination becomes less possible. The observed changes in the profiles of fluorescence spectra at different durations of heating can be attributed to the changes in the morphology (size and surface structure) of the nanoparticles. It seems that change in the pyrolysis time induced a change in the morphology of the CdS nanoparticulates as well as a significant decrease in the particle size. Hence particle size could be controlled by varying the duration of pyrolysis.

The X-ray powder diffraction data for samples obtained by pyrolysis of the complexes were compared with those for samples prepared by the wet synthetic method. The two powder

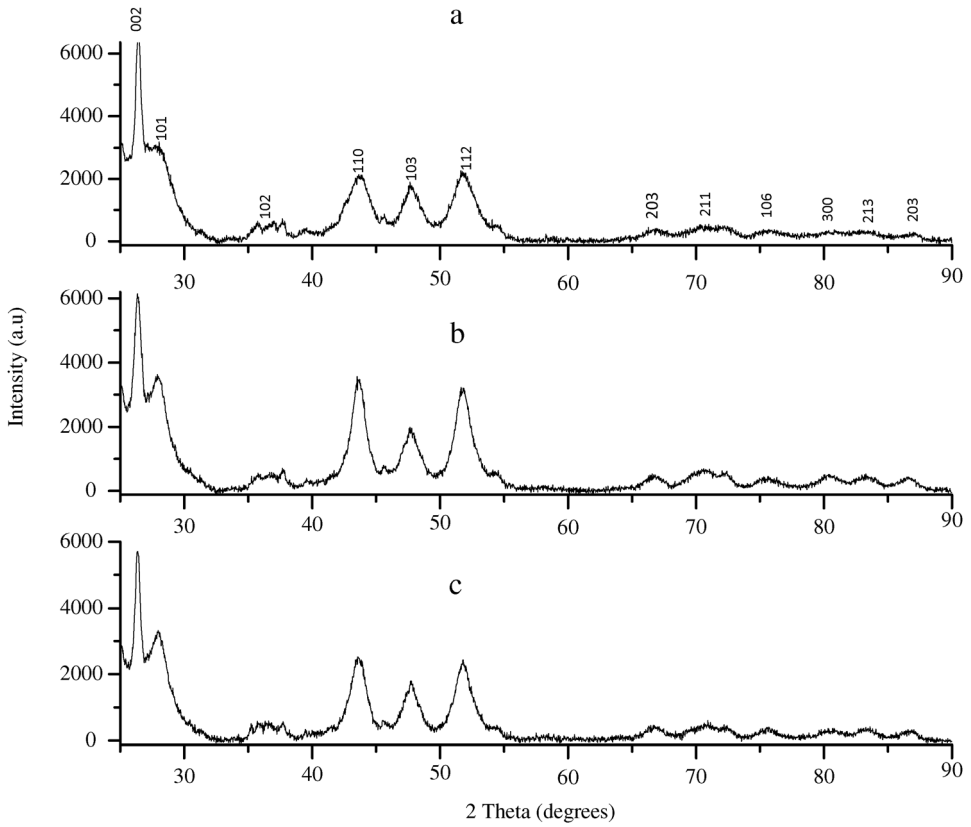

Fig. 11 X-ray powder diffraction patterns of CdS nanoparticles grown in HDA ligand solution at 185 °C, 1 h; complex (a) **1** (b) **2** and (c) **3**, respectively.

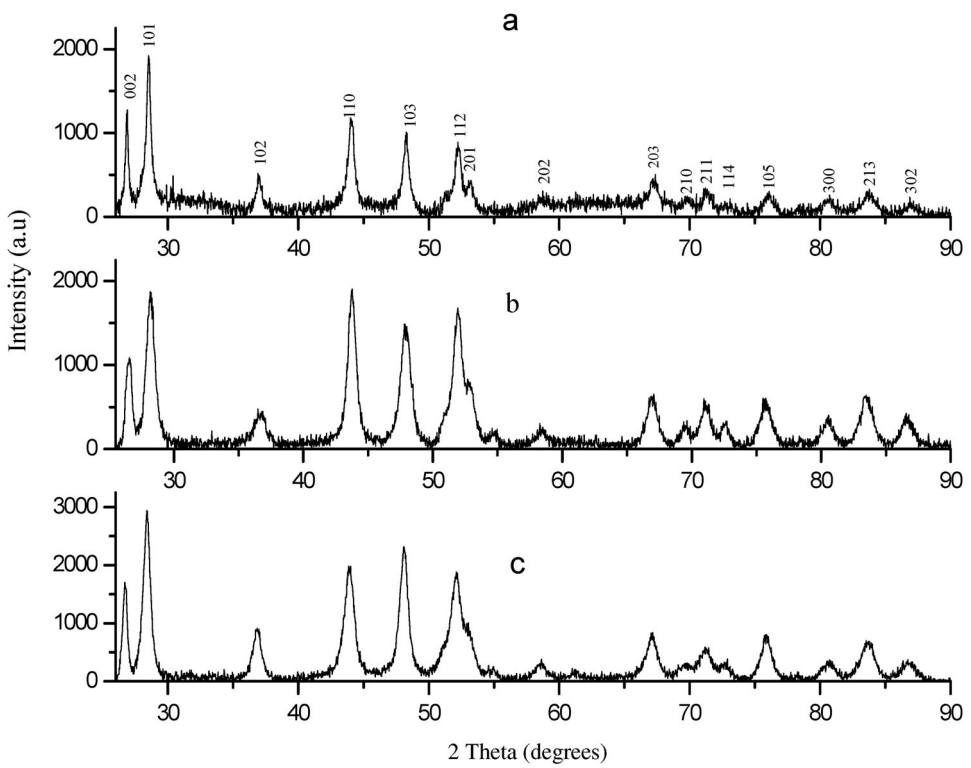

Fig. 12 Powder X-ray diffraction patterns of CdS nanoparticles obtained by the pyrolysis of complex (a) **1** (b) **2** and (c) **3**, respectively, in a furnace at 350 °C under nitrogen flow for 1 h.

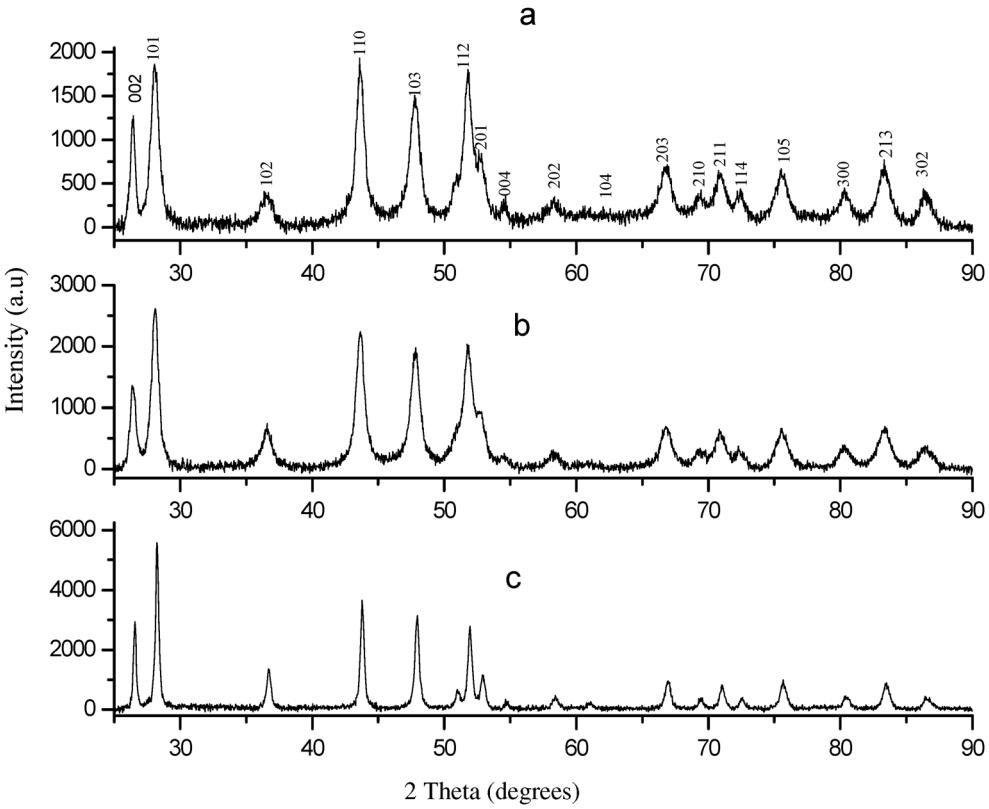

Fig. 13 X-ray powder diffraction patterns of CdS nanoparticles obtained by the pyrolysis of complex (a) **1**, (b) **2** and (c) **3**, respectively, in a furnace at 350 °C under nitrogen flow for 2 h.

patterns were identical. XRD patterns of the three HDA-capped CdS are shown in Fig. 11. All the patterns show well defined broad peaks, which confirm the high nanocrystalline nature of the samples. Moreover, these patterns confirm that the synthesized CdS nanoparticles are of hexagonal greenockite type (JCPDS Powder Diffraction File no. 041-1049). The pyrolysis of complexes **1**, **2** and **3**, carried out at 350 °C, for 1 and 2 h showed similar phases as represented in Fig. 12 and 13. The residues were also identified as crystalline hexagonal-phased cadmium sulphide with the strong characteristic (110), (103), (112) peaks. The XRD patterns show obviously broadened diffraction peaks in the nanoparticles prepared by a wet process compared to those by pyrolysis, signifying the more finite size of these crystallites. The stronger and narrower (002) peak of the solvothermally prepared particles (Fig. 11) indicates that the nanocrystals were elongated along the *c*-axis.[40,41]

Conclusion

Three new single source precursors have been used for a controlled synthesis of cadmium sulphide nanoparticles. The preparation of the nanoparticles was achieved *via* pyrolysis and solvolysis in the presence of hexadecylamine. Surface passivation of the CdS nanoparticles resulted in carrier confinement and improved optical properties. The results show that the method used for the nanoparticles synthesis has a significant effect on the morphology and the optical properties of the final materials. The presence of 2,2′-bipyridine and 1,10-phenanthroline in the precursor affects the axial growth of CdS nanoparticles.

Acknowledgements

The financial support from the National Research Foundation (NRF), South Africa, and North West University, Potchefstroom, South Africa, is gratefully acknowledged. The authors are grateful to M. A. Jaffer of Electron Microscopy Unit UCT for TEM analyses.

References

1 M. Pattabi and J. Uchil, *Sol. Energy Mater. Sol. Cells*, 2000, **63**, 309–314.
2 J. Frenzel, J.-O. Joswig and G. Seifert, *J. Phys. Chem. C*, 2007, **111**, 10761–10770.
3 S. R. Stebbing, R. W. Hughes and P. A. Reynolds, *Adv. Colloid Interface Sci.*, 2009, **147**, 272–280.
4 R. Maity and K. K. Chattopadhyay, *J. Nanopart. Res.*, 2006, **8**, 125–130.
5 A. P. Alivisatos, *Science*, 1996, **271**, 933–937.
6 W. Yu and X. Peng, *Angew. Chem., Int. Ed.*, 2002, **41**, 2368–2371.
7 J. S. Jie, W. J. Zhang, Y. Jiang, X. M. Meng, Y. Q. Li and S. T. Lee, *Nano Lett.*, 2006, **6**, 1887–1892.

8 Q. Wang, G. Xu and G. Han, *J. Solid State Chem.*, 2005, **178**, 2680–2685.
9 X. Ma, F. Xu and Z. Zhang, *Mater. Res. Bull.*, 2005, **40**, 2180–2188.
10 Y. Wang, C. Y. To and D. H. L. Ng, *Mater. Lett.*, 2006, **60**, 1151–1155.
11 A. V. Murugan, R. S. Sonawane, B. B. Kale, S. K. Apte and A. V. Kulkarni, *Mater. Chem. Phys.*, 2001, **71**, 98–102.
12 M. Kristl, I. Ban, A. Danc, V. Danc and M. Drofenik, *Ultrason. Sonochem.*, 2010, **17**, 916–922.
13 C. Bao, M. Jin, R. Lu, P. Xue, Q. Zhang, D. Wang and Y. Zhao, *J. Solid State Chem.*, 2003, **175**, 322–327.
14 P. J. Wright, B. Cockayne, A. C. Jones, E. D. Orell, P. O'Brien and O. F. Z. Khan, *J. Cryst. Growth*, 1989, **94**, 97–101.
15 P. J. Wright, B. Cockayne, P. J. Parbrook, P. E. Oliver and A. C. Jones, *J. Cryst. Growth*, 1991, **108**, 525–533.
16 J. B. Mullin, D. J. Cole-Hamilton, S. J. C. Irvine, J. E. Hails, J. Giess and J. S. Gough, *J. Cryst. Growth*, 1990, **101**, 1–13.
17 P. Bera, C.-H. Kim and S. Seok, *Solid State Sci.*, 2010, **12**, 1741–1747.
18 D. Fan, M. Afzaal, M. A. Mallik, C. Q. Nguyen, P. O'Brien and P. J. Thomas, *Coord. Chem. Rev.*, 2007, **251**, 1878–1888.
19 N. L. Pickett and P. O'Brien, *Chem. Rec.*, 2001, **1**, 467–479.
20 W. S. Rees, Jr. and G. Krauter, *J. Mater. Res.*, 1996, **11**, 3005–3016.
21 M. Green and P. O'Brien, *Adv. Mater. Opt. Electron.*, 1997, **7**, 277–279.
22 G. Kedarnath, V. K. Jain, S. Ghoshal, G. K. Dey, C. A. Ellis and E. R. T. Tiekink, *Eur. J. Inorg. Chem.*, 2007, 1566–1576.
23 D. C. Onwudiwe and P. A. Ajibade, *Polyhedron*, 2010, **29**, 1431–1436.
24 P. A. Ajibade and D. C. Onwudiwe, *J. Mol. Struct.*, 2013, **1034**, 249–256.
25 J. D. S. Newman and G. J. Blanchard, *Langmuir*, 2006, **22**, 5882–5887.
26 T. Mishra, R. K. Sahu, S. H. Lim, L. G. Salamanca-Riba and S. Bhattacharjee, *Mater. Chem. Phys.*, 2010, **123**, 540–545.
27 M. Chen, Y. G. Feng, X. Wang, T. C. Li, J. Y. Zhang and D. J. Qian, *Langmuir*, 2007, **23**, 5296–5304.
28 B. S. Zou, R. B. Little, J. P. Wang and M. A. El-Sayed, *Int. J. Quantum Chem.*, 1999, **72**, 439–450.
29 D. J. Elliot, K. Grieve, D. N. Furlong and F. Grieser, *Adv. Colloid Interface Sci.*, 2001, **91**, 113–158.
30 Y. S. Fu, X. W. Du, S. A. Kulinich, J. S. Qiu, W. J. Qin, R. Li, J. Sun and J. Liu, *J. Am. Chem. Soc.*, 2007, **129**, 16029–16033.
31 M. G. Bawendi, P. J. Carroll, W. L. Wilson and L. E. Brus, *J. Chem. Phys.*, 1992, **96**, 946–954.
32 V. Singh, P. K. Sharma and P. Chauhan, *Mater. Charact.*, 2011, **62**, 43–52.
33 M. N. Kalasand, M. K. Rabinal and B. G. Mulimani, *J. Phys. D: Appl. Phys.*, 2010, **43**, 305301.
34 H. Yang, C. Huang, X. Li, R. Shi and K. Zhang, *Mater. Chem. Phys.*, 2005, **90**, 155–158.
35 Y. Wada, H. Kuramoto, J. Anand, T. Kitamura, T. Sakata, H. Mori and S. Yanagida, *J. Mater. Chem.*, 2001, **11**, 1936–1940.
36 K. S. Babu, C. Vijayan and P. Haridoss, *Mater. Lett.*, 2006, **60**, 124–126.
37 N. V. Deshmukh, T. M. Bhave, A. S. Ethiraj, S. R. Sainkar, V. Ganesan, S. V. Bhoraskar and S. K. Kulkarni, *Nanotechnology*, 2001, **12**, 290–294.
38 P. S. Nair, M. M. Chili, T. Radhakrishnan, N. Revaprasadu, P. Christian and P. O'Brien, *S. Afr. J. Sci.*, 2005, **101**, 466–470.
39 Y. Jun, J. H. Lee, J. Choi and J. Cheon, *J. Phys. Chem. B*, 2005, **109**, 14795–14806.
40 Y. Li, X. Li, C. Yang and Y. Li, *J. Phys. Chem. B*, 2004, **108**, 16002–16011.
41 L. Jiang, M. Yang, S. Zhu, G. Pang and S. Feng, *J. Phys. Chem. C*, 2008, **112**, 15281–15284.

